

Heterodyne measurement of Wigner distributions for classical optical fields

K. F. Lee, F. Reil, S. Bali, A. Wax, and J. E. Thomas

Department of Physics, Duke University, Durham, North Carolina 27708-0305

Received May 24, 1999

We demonstrate a two-window heterodyne method for measuring the x - p cross correlation, $\langle E^*(x)E(p) \rangle$, of an optical field E for transverse position x and transverse momentum p . This scheme permits independent control of the x and p resolution. A simple linear transform of the x - p correlation function yields the Wigner phase-space distribution. This technique is useful for both coherent and low-coherence light sources and may permit new biological imaging techniques based on transverse coherence measurement with time gating. We point out an interesting analogy between x - p correlation measurements for classical-wave and quantum fields. © 1999 Optical Society of America

OCIS codes: 000.1600, 030.1640, 270.6570, 170.3880.

Wigner distribution functions provide a complete description of the coherence properties of classical-wave fields. Hence they have important applications in fundamental studies of light propagation and tomographic imaging. For a classical field $E(x)$ varying in one spatial dimension, the Wigner phase-space distribution is Fourier transform related to the mutual coherence function¹

$$W(x, p) = \int \frac{d\epsilon}{2\pi} \exp(i\epsilon p) \langle E^*(x + \epsilon/2)E(x - \epsilon/2) \rangle. \quad (1)$$

Here x is a transverse position, p is a transverse wave vector (momentum) in the x direction, and $\langle \dots \rangle$ denotes a statistical average. Wigner functions have been used to display the time-frequency dependence of classical fields,² although they are not generally positive definite.³ The Wigner distribution function plays a role that is closely analogous to a classical phase-space distribution in position and momentum, permitting an intuitive particlelike description of the underlying wave propagation.

In this Letter we show that Wigner distributions for classical optical fields can be determined by use of a novel two-window heterodyne detection scheme. The signal field is mixed with a local-oscillator (LO) field comprising a coherent superposition of a tightly focused beam and a highly collimated beam. This scheme permits independent control of the x and p resolution, permitting concurrent localization of x and p with a variance product that surpasses the minimum uncertainty limit associated with Fourier-transform pairs.² The method can be applied with low-coherence light, permitting time gating to be combined with Wigner function measurement, thereby permitting new venues for biomedical coherence tomography. We also show that an interesting analogy exists between our choice of LO field and that employed in a recent quantum-teleportation experiment.⁴

We previously described the measurement of smoothed Wigner phase-space distributions for classical fields by use of balanced heterodyne measurement of the mean-square beat amplitude $\langle |V_B|^2 \rangle$.⁵ The

mean-square beat amplitude is proportional to the square of the magnitude of the spatial overlap integral of the LO and signal fields in the detector planes, D1 and D2, shown in Fig. 1. By use of Fourier optics, it is straightforward to show that⁵

$$\langle |V_B(d_x, d_p)|^2 \rangle \propto \int dx dp W_{LO}(x - d_x, p + kd_p/f) W_S(x, p). \quad (2)$$

Here $W_S(x, p)[W_{LO}(x, p)]$ is the Wigner distribution, given by Eq. (1), of the signal (LO) field in the input planes of lenses L2 (L1). The y integration is suppressed for simplicity. Relation (2) shows that the mean-square beat signal yields a phase-space contour plot of $W_S(x, p)$ with phase-space resolution determined by W_{LO} . For a Gaussian LO beam the position resolution is determined by the diameter of the LO beam, whereas the momentum resolution is determined by the corresponding diffraction angle. Hence the phase-space resolution is minimum uncertainty limited, and the measured Wigner distribution is smoothed.⁶ The system scans the LO position over a distance $d_x = \pm 1$ cm by translating mirror M1 in the LO path. The LO momentum is scanned over $\pm 0.3 k$, where $k = 2\pi/\lambda$ is an optical wave vector, by

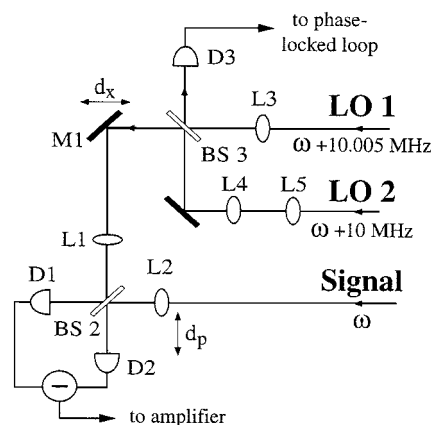


Fig. 1. Scheme for two-window heterodyne measurement of Wigner distributions. See text for definitions.

translation of signal-beam input lens L2 (focal length $f = 6$ cm) by a distance d_p .⁵

Heterodyne measurement with coherent light has been used to measure smoothed Wigner phase-space distributions for small-angle scattering in a multiple-scattering medium.⁷ The use of low-coherence light⁸ permits selection of optical paths in the scattering medium. This selectivity has permitted measurements of phase-space distributions for low-order scattered light in transmission^{9,10} as well as for coherent backscatter,¹¹ with subfemtowatt sensitivity and a dynamic range of 13 orders of magnitude.

However, heterodyne measurement with a single LO field does not permit independent control of the position and momentum resolutions. One can achieve independent control by measuring the mutual coherence of the signal field, using shearing interferometry and Fourier transformation to obtain the Wigner function.¹² Using this method, Cheng and Raymer measured mutual coherence in a multiple-scattering medium to explore a classical-wave analog of quantum decoherence.¹³ However, since this method does not rely on a reference field, one cannot readily extend it to distinguish optical path lengths by exploitation of low-coherence light sources.

To obtain independent control of the x and p resolution in a heterodyne measurement, we employ a slowly varying LO field of the form

$$\mathcal{E}_{\text{LO}}(x) = \mathcal{E}_0 \left[\exp\left(-\frac{x^2}{2a^2}\right) + \beta \exp\left(-\frac{x^2}{2A^2}\right) \exp(i\theta) \right], \quad (3)$$

Here a is chosen to be small compared with the distance scales of interest and $1/A$ is chosen to be small compared with the momentum scales of interest in the signal field. We take $A^2 \gg a^2$. In this case the phase- (θ -) dependent part of the Wigner function for the LO takes the form

$$\begin{aligned} W_{\text{LO}}(x, p) &\propto \exp\left(-\frac{2x^2}{A^2} - 2a^2p^2\right) \cos(2xp + \theta) \\ &\simeq \cos(2xp + \theta), \end{aligned} \quad (4)$$

where the last form assumes that the range of the momentum and position integration in relation (2) is limited by the signal field.

In the experiments, as illustrated in Fig. 1, the LO beam is obtained by combination of two fields that differ in frequency by 5 kHz, so that $\theta = (2\pi \times 5 \text{ kHz})t$. Lens L3 focuses beam LO1 to a waist of width a , and lenses L4 and L5 expand beam LO2 to width A . We combine these two components at beam splitter BS 3 to obtain a LO field of the form given in Eq. (3). We monitor one output of the beam splitter with detector D3 to phase lock the 5-kHz beat signal to the reference channel of a lock-in amplifier. Each component of the LO beam is shaped so that it is at a beam waist at the input plane of the heterodyne imaging system (lens L1). The dual LO and signal fields are mixed at BS 2, and the rms beat amplitude at 10 MHz is measured with an analog spectrum ana-

lyzer. The spectrum analyzer bandwidth, 100 kHz, is chosen to be large compared with the 5-kHz difference frequency. The output of the spectrum analyzer is squared in real time with a low-noise multiplier, the output of which is sent to the lock-in amplifier. The lock-in outputs for the in- and out-of-phase quadratures then directly determine the real and the imaginary parts of the quantity

$$\begin{aligned} S(x_0, p_0) &= \int \frac{dx' dp'}{\pi} \exp[2i(x' - x_0) \\ &\quad \times (p' - p_0)] W_S(x', p') \\ &= \langle \mathcal{E}^*(x_0) \mathcal{E}(p_0) \rangle \exp(ix_0 p_0). \end{aligned} \quad (5)$$

Here $x_0 = d_x$ is the center position of the LO fields and $p_0 = -kd_p/f$ is the center momentum. As the position of mirror M1 is scanned a distance d_x , the optical path lengths of the LO fields change. For the current experiments the change in path lengths is small compared with the Rayleigh length and the coherence length of the beams, so translating M1 simply changes the center position of the LO fields. When this is not the case, lens L3 can be moved in conjunction with M1 so that the beam waist is kept at L1. We can add a corner reflector in the LO arm before splitting it into LO 1 and LO 2 to keep the optical path length constant as M1 is scanned. This is an important consideration when one is using low-coherence light.⁸

Equation (5) defines the Margenau–Hill distribution of the signal field. Equation (5) gives the correlation between the field component at position x_0 with the field component of momentum p_0 . Both the Margenau–Hill and Wigner functions belong to the Cohen class of functions. It is known that one can easily transform a function in the Cohen class to yield any other function in that class.² Thus we can readily invert the detected signal given in Eq. (5) to obtain the Wigner function by a linear transformation. Using the reality of $W_S(x, p)$, we obtain

$$\begin{aligned} W_S(x, p) &= \int \frac{dx_0 dp_0}{\pi} \cos[2(x - x_0)(p - p_0)] \\ &\quad \times S_R(x_0, p_0) + \int \frac{dx_0 dp_0}{\pi} \sin[2(x - x_0)(p - p_0)] \\ &\quad \times S_I(x_0, p_0), \end{aligned} \quad (6)$$

where S_R and S_I are the real and the imaginary parts of Eq. (5), i.e., the in- and out-of-phase lock-in signals.

As an initial demonstration of the capability of this system, we measure the Wigner function for an ordinary Gaussian beam. The signal beam is shaped by a telescope so that its waist coincides with input plane L2 of the heterodyne imaging system. For a Gaussian beam at its waist, Eq. (1) gives the Wigner distribution as $W_S(x, p) = (1/\pi) \exp(-x^2/w^2 - w^2p^2)$, where $w = 0.85$ mm is the $1/e$ -intensity width. The x - p correlation function for the signal field is measured by use of a LO beam of the form given by Eq. (3) with $a = 81 \mu\text{m}$, $A = 2.6$ mm, and $\beta = 1$. The real and

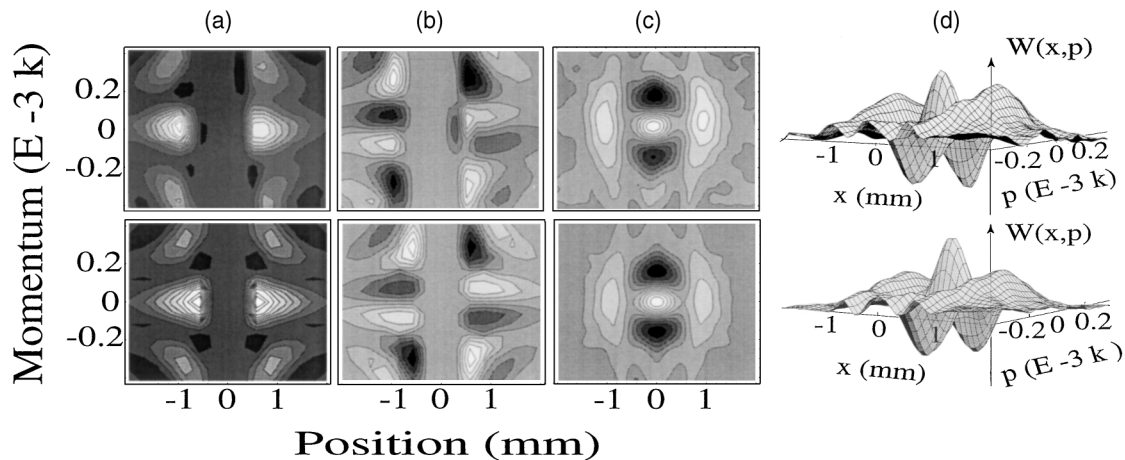


Fig. 2. Measured Wigner distribution for a Gaussian signal beam obscured by a wire: (a) in-phase lock-in signal $S_R(x, p)$, (b) out-of-phase lock-in signal $S_I(x, p)$, (c) recovered Wigner distribution showing negative regions. Note that the position distribution $\int dp W(x, p) = 0$ for x near the wire, as it should. (d) Three-dimensional view of recovered Wigner distribution. Top, data; bottom, theoretical prediction.

the imaginary parts of the detected signal, Eq. (5), are used in Eq. (6) to recover the Wigner distribution of the signal field. We χ^2 fit the width of the measured in-phase signal in position for $p = 0$ to obtain a spatial width $w = 0.87 \pm 0.05$ mm, whereas the corresponding momentum distribution for $x = 0$ yields $w = 0.83 \pm 0.05$ mm. Both results are in excellent agreement with the measured width $w = 0.85$ mm obtained by use of a diode array, demonstrating that high position and momentum resolution can be jointly obtained.

A more interesting example is the Wigner function for the same Gaussian beam with a wire placed at its center in input plane L2. In this case the slowly varying field is Gaussian as before but multiplied by a slit function that sets the field equal to zero for $|x| \leq 0.5$ mm. Figures 2(a) and 2(b) show contour plots of the real and the imaginary parts of the detected signal (top row) and the corresponding predicted distributions (bottom row), respectively. We can use the two measured distributions in Eq. (6) to determine the Wigner distribution for the field, illustrated in Fig. 2(c). An interesting feature of this distribution is the oscillation in momentum for $x = 0$, the position of the wire. This feature can be seen in Fig. 2(d), in which the inverted data are shown as a three-dimensional plot (top) and compared with the predicted distribution (bottom).

We note that an interesting analogy exists between the small and the large beams of our two-window LO and the superposition of the position (in-phase) and the momentum (out-of-phase) squeezed fields that were used to determine the quantum Wigner function in a recent teleportation experiment.⁴ To elucidate this analogy we consider a suitably chosen lenslike medium,¹⁴ the transverse modes of which provide a natural harmonic-oscillator basis. A Gaussian beam of the same size as the lowest mode but displaced in transverse position and momentum corresponds to a coherent state, whereas Gaussian beams of smaller (larger) size than the lowest mode correspond to position (momentum) squeezed states. New insights can

be realized by exploration of additional analogies between classical and quantum optics.¹⁵

In conclusion, we have demonstrated two-window heterodyne measurement of the Wigner function for an optical field, with independent control of the x and p resolution. We are currently applying this technique with low-coherence light sources for time-gated studies of coherence propagation in multiple-scattering media.

The research was supported by the National Institutes of Health and the National Science Foundation. J. E. Thomas's e-mail address is jet@phy.duke.edu.

References

1. M. Hillery, R. F. O'Connell, M. O. Scully, and E. P. Wigner, *Phys. Rep.* **106**, 121 (1984).
2. L. Cohen, *Time-Frequency Analysis* (Prentice-Hall, Englewood Hills, N.J., 1995).
3. P. J. Loughlin, J. W. Pitton, and L. E. Atlas, *IEEE Trans. Signal Process.* **42**, 2696 (1994).
4. A. Furusawa, J. L. Sørensen, S. L. Braunstein, C. A. Fuchs, H. J. Kimble, and E. S. Polzik, *Science* **282**, 706 (1998).
5. A. Wax and J. E. Thomas, *Opt. Lett.* **21**, 1427 (1996).
6. N. D. Cartwright, *Physica A* **83**, 210 (1976).
7. A. Wax and J. E. Thomas, *J. Opt. Soc. Am. A* **15**, 1896 (1998).
8. A. Wax, S. Bali, and J. E. Thomas, *Opt. Lett.* **24**, 1188 (1999).
9. A. Wax and J. E. Thomas, *Proc. SPIE* **3598**, 2 (1999).
10. A. Wax and J. E. Thomas, *Proc. SPIE* **3726**, 494 (1999).
11. A. Wax, "Optical phase space distributions for coherence tomography," Ph.D. dissertation (Duke University, Durham, N.C., 1999).
12. C. Iaconis and I. A. Walmsley, *Opt. Lett.* **21**, 1783 (1996).
13. C.-C. Cheng and M. G. Raymer, *Phys. Rev. Lett.* **82**, 4807 (1999).
14. A. Yariv, *Introduction to Optical Electronics* (Holt, Rinehart & Winston, New York, 1976), Chap. 3, pp. 29–57.
15. K. Wódkiewicz and G. H. Herling, *Phys. Rev. A* **57**, 815 (1998); N. J. Cerf, C. Adami, and P. G. Kwiat, *Phys. Rev. A* **53**, R1477 (1998).